Laccaria bicolor MiSSP8 is a small-secreted protein decisive for the establishment of the ectomycorrhizal symbiosis

Clément Pellegrin[1,2,§], Yohann Daguerre[1,2,⊡], Joske Ruytinx[1,2,*], Frédéric Guinet[1,2], Minna Kempainnen[3], Mélodie B. Plourde[4], Arnaud Hecker[1,2], Emmanuelle Morin[1,2], Alejandro G. Pardo[3], Hugo Germain[4], Francis M. Martin[1] & Claire-Veneault-Fourrey[1,2]

Affiliations

[1] INRA, UMR 1136, Interactions Arbres/Microorganismes (IAM), Centre INRA de Nancy, Champenoux, France

[2] Université de Lorraine, UMR 1136, Interactions Arbres/Microorganismes (IAM), Faculté des Sciences, Vandœuvre lès Nancy, France

[3] Laboratorio de Micología Molecular, Departamento de Ciencia y Tecnologıa, Universidad Nacional de Quilmes and CONICET, Roque Sáenz Peña 352, B1876 Bernal, Provincia de Buenos Aires, Argentina

[4] Departement de Chimie, Biochimie, Physique, Université du Québec à Trois-Rivières, 3351 boulevard des Forges, Trois-Rivières, QC, G9A 5H7, Canada

§ Current address: Max Planck Institute for Terrestrial Microbiology, Karl-von-Frisch Str. 10, 35043 Marburg, Germany

⊡Current address: Umeå Plant Science Centre, Department of Forest Genetics and Plant Physiology, Swedish University of Agricultural Sciences, 901 83 Umeå, Sweden

* Current address: Hasselt University, Centre for Environmental Sciences, Agoralaan building D, 3590 Diepenbeek, Belgium

Corresponding author: claire.fourrey@univ-lorraine.fr; Phone: +33 (0)383394081

Keywords: ectomycorrhizal; hyphal aggregation; repetitive motif; symbiosis; small-secreted protein.

1

Summary

- The ectomycorrhizal symbiosis is a predominant tree-microbe interaction in forest ecosystems sustaining tree growth and health. Its establishment and functioning implies a long-term and intimate relationship between the soil-borne fungi and the roots of trees. Mycorrhiza-induced Small Secreted Proteins (MiSSPs) are hypothesized as keystone symbiotic genes, required to set up the symbiosis by modifying the host metabolism and/or building the symbiotic interfaces.

- Since *L. bicolor MiSSP8* is the third most highly induced MiSSPs in symbiotic tissues and it is expressed in fruiting bodies, we report its functional study by analysing phenotypes of *L. bicolor MiSSP8*-RNAi mutants and MiSSP8 *in planta* subcellular localization.

- The *MiSSP8*-RNAi knockdown mutants are impaired in their mycorrhization ability with *Populus*, with the lack of fungal mantle and Hartig net development. When expressed heterologously *in planta*, MiSSP8 shows a punctate localization that partially colocalize with plasmodesmata. Moreover, MiSSP8 displays a fungal-specific repetitive motif, present in proteins from both saprotrophic and ectomycorrhizal fungi.

- MiSSP8 is a *Laccaria*-specific small-secreted protein required for early stages of ectomycorrhizal symbiosis. Our data suggest that MiSSP8 has a possible dual role: one in basic fungal biology regulating hyphal aggregation and another *in planta*, related to its plasmodesmata co-localization.

2

Introduction

Forest soils contain a wide diversity of microorganisms displaying multiple nutrition modes from saprotrophy to pathogenicity, through mutualism (Buée et al., 2009; Uroz et al., 2010; Fierer et al., 2007). Tree-associated microbes are considered as key drivers of tree health, productivity, and ecosystem functionality (Berg et al., 2014 ; 2015). In particular, fungal communities are primary contributors to carbon and nitrogen cycling in forest ecosystems (van der Heijden, 1998; Lindahl and Tunlid, 2015). Trees forming ectomycorrhizae (ECM) with soil-borne fungi dominate northern forest ecosystems (Brundrett, 2009). These mutualistic interactions rely on bidirectional exchanges of nutrients, which happen on mycorrhized roots. The host tree provides carbon derived from its photosynthesis to the fungus, whereas in return ECM fungi provide nitrogen, phosphorous and water. Ectomycorrhizal fungi thus inhabit a dual ecological niche, forest soils and tree root cells, requiring two contrasting ways of life: decomposers in soil and biotrophic within plant living tissues. However, most ECM fungi develop (i) extramatrical mycelium exploring the rhizospheric surrounding soil, (ii) aggregated fungal hyphae ensheathing fine lateral roots named mantle, and finally (iii) a highly branched network of fungal hyphae (called the Hartig net) within the apoplastic space of cortical root cells (Martin et al., 2016). The Hartig net constitutes the biotrophic interface required for efficient nutrient exchanges. In particular environmental conditions (humidity, temperature), host-derived carbon can be used to build the fruiting body, a spore-releasing structure made of hyphal aggregation (Genre & Bonfante, 2012; Lakkireddy et al., 2011).

Despite their critical ecological roles, only few ECM interactions were studied at the molecular level. Notably, mechanisms mediating ECM symbiosis remain mostly uncharacterized. Nevertheless, recent reviews proposed a model for the establishment of ectomycorrhizal symbioses (Daguerre et al., 2016; Martin et al., 2016). First, a pre-contact phase during which plant and fungi communicate is a prerequisite for successful root colonization. Diffusible molecules such as fungal auxins, sesquiterpenes, likely mediate this

3

communication and trigger an increase of the lateral roots formation (Felten et al., 2009; Ditengou et al., 2015; Krause et al., 2015; Vayssières et al., 2015). Then, fungal accommodation within the apoplast of cortical root cells requires controlling both hyphal and host root development (Martin et al., 2016). For example, in poplar-*L. bicolor* model, both ethylene and jasmonic acid treatment restrict *in planta* fungal colonization i.e. restrict the intraradicular hyphal network (Plett et al., 2014). The symbiotic interface at the Hartig net derives from remodelling of both fungal and plant cell walls (Balestrini and Kottke, 2016). Cell wall carbohydrates and proteins (e.g. hydrophobins, mannoproteins) are thus likely to actively contribute for *in planta* fungal colonisation (for review, Balestrini and Kottke, 2016) and for efficient nutrient exchanges. Formation of the Hartig net also leads to a massive fungal colonization within the apoplast of colonized roots, without eliciting strong defence responses (Martin et al., 2016). Considering ECM symbiosis as a biotrophic plant-fungal interaction, secreted fungal molecules likely govern plant colonization by subverting host immunity and manipulating its metabolism to promote the symbiosis establishment and/or functioning (Plett & Martin, 2015; Lo Presti et al., 2015).

Genome-wide analysis of *Laccaria bicolor* led to the identification of 98 proteins, named MiSSPs (Mycorrhiza-induced Small Secreted Proteins), up-regulated in symbiotic tissues (Martin et al., 2008). Among them, only MiSSP7 from *L. bicolor* was described as a symbiosis effector. MiSSP7 is secreted by the fungus, enters the host cells, in which it localizes within the nucleus. Moreover, *MiSSP7*-RNAi mutants are impaired in ectomycorrhiza formation (Plett et al., 2011). Inside the nucleus, MiSSP7 interacts with the *Populus trichocarpa* PtJAZ6 (JAsmonate Zim domain 6), a co-receptor of jasmonic acid (Plett et al., 2014). MiSSP7 stabilizes PtJAZ6, avoiding its degradation in the presence of jasmonic acid, leading to the repression of target genes' transcription (Plett et al., 2014). Preliminary results have showed that genes involved in plant cell wall remodelling and plant defence responses might be the target genes (Plett et al., 2014). Furthermore, effector proteins, such as SP7 from the endomycorrhizal fungus *Rhizophagus irregularis* (Kloppholz et al., 2011), as well as PIIN_08944 and FGB1 (Fungal Glucan-Binding 1, PIIN_03211) from the root endophyte *Piriformospora indica* (Akum et al., 2015; Wawra et al., 2016) also

4

suppress host immunity promoting root colonization and symbiosis. These data support the concept whereby a mutualistic symbiont uses its repertoire of secreted proteins to set up the symbiosis by suppressing host immunity and/or targeting cell-wall remodelling.

Considering the diversity of secreted proteins used by pathogens to alter the host metabolism, mycorrhizal fungi might use an equivalent strategy to setup their interaction. However, available literature on such proteins required for the symbiosis establishment is still very poor and functional analyses of MiSSPs are required to clarify and detail how mycorrhizal fungi coordinate their activity with their host plant (Plett & Martin, 2015). The Mycorrhiza-induced Small Secreted Protein of 8 kDa, i.e MiSSP8 (JGIv2 ID #388224 ; JGIv1 ID #298667), displays the third highest induction in mature ectomycorrhizal root tips and is also up-regulated in fruiting-bodies (Martin et al., 2008). MiSSP8 is part with other MiSSPs of the "core" regulon expressed during the colonization of two hosts, *Populus trichocarpa* and *Pseudotsuga menziesii* (Plett et al., 2015a). The proteins associated to this core regulon have hence been hypothesized to be key genetic determinants required for the symbiosis development in *L. bicolor* (Plett et al., 2015a). In this study, we report the functional analysis of *L. bicolor* MiSSP8 by using a combination of experimental and *in silico* approaches. We identify MiSSP8 as a key symbiosis factor required for *L. bicolor* mycorrhization ability, mantle formation and subsequent Hartig net development. This symbiosis factor contains a repetitive motif which seems fungal specific, as we found it only in fungal proteomes, mostly in proteins of ECM and saprotrophic fungi. In addition, when transiently expressed *in planta*, MiSSP8 partially co-localizes to plasmodesmata and this localization does not depend on binding on callose, suggesting a dual role for this protein.

Material and methods

Microorganism and plant material

Saccharomyces cerevisiae strains YTK12 (Jacobs et al., 1997), MaV103 and MaV203 (Invitrogen) were propagated on YAPD medium (1% yeast extract, 2% peptone, 2% glucose, and 40 mg/L adenine) and cultured at 30°C. The ectomycorrhizal fungus *L. bicolor* strains (S238N, Maire P. D. Orton and RNAi-lines) were maintained at 25°C on modified

5

Pachlewski medium P5 +/- $150\mu g.ml^{-1}$ of hygromycin B (Pachlewski & Pachlewskia, 1974). The hybrid *Populus tremula x Populus alba* (clone INRA 717-1-B4) cuttings were micropropagated *in vitro* and grown on half MS medium (Murashige & Skoog, 1962) in glass culture tubes under a 16 h photoperiod at 24°C in a growth chamber. *Nicotiana benthamiana* plants were grown from seeds at 22°C under 16 hours photoperiod for 4 to 6 weeks before used in *Agrobacterium*-transformation. *L. bicolor* sporocarps were harvested from a nursery experiment of inoculated Douglas firs. We harvested three samples for two developmental stages. "Early" stage corresponds to just emerging fruiting body and "late" stage corresponds to fruiting body with "open" cap. For each developmental stage, we divided the sporocarps into stipe and cape, prior to RNAs extraction (Fig. S2).

Yeast secretion trap assay

Functional validation of the predicted signal peptide of MiSSP8 was done using the yeast signal-sequence trap assay (Plett et al., 2011). Briefly, full-length sequences of MiSSP8 with or without its signal peptide were cloned into pSUC2-GW plasmid carrying the invertase, *SUC2*, lacking both its initiation methionine and signal peptide. Yeast strain YTK12 was transformed with 200 ng of the plasmid using the lithium acetate method (Gietz & Schiestl, 2007). All transformants were confirmed by PCR with vector-specific primers and grown on yeast minimal medium with glucose (SD-W medium: 0.67% Yeast Nitrogen Base without amino acids, 0.075% tryptophan dropout supplement, 2% glucose and 2% agar). To assess invertase secretion, overnight yeast cultures were diluted to an $O.D_{600} = 1$ and 20 µl of dilution were plated onto YPSA medium (1% yeast extract, 2% peptone, 2% sucrose, and 1 $\mu g.mL^{-1}$ antimycin A, inhibitor of cytochrome c oxidase). The YTK12 strains transformed with either the pSUC2-GW empty vector or containing SUC2SP (yeast invertase with signal peptide) were used as negative and positive controls, respectively.

Genetic transformation of L. bicolor

The ihpRNA expression cassette/transformation vector was constructed using the pHg/SILBAγ vector system (Kemppainen et al, 2005; Kemppainen & Pardo, 2010). The full-lenght MiSSP8 cDNA was amplified from oligo(dT)18 synthesized S238N cDNA (First Strand cDNA Kit, (Fermentas) using the following gene specific primers:

6

MISSP8-*Sna*BIFor: CTTCTACGTAATGTATTTCCACACTCTTTTCG

MISSP8-*Hind*IIIRev: TGTCAAGCTTTCAATCACTATCGCGCCTC.

The cDNA was TA-cloned into pCR®2.1-TOPO® (Invitrogen) for sequencing and the corresponding plasmid was used as PCR template to obtain the amplicons needed for ihpRNA expression cassette construction. The cloning into the pSILBAy vector was carried out using the *Sna*BI, *Hind*III, *Bgl*II and *Stu*I restriction sites in pSILBAy. Primers used for amplification of the MiSSP8 sequence arms were:

MISSP8-*Sna*BIFor: CTTCTACGTAATGTATTTCCACACTCTTTTCG

MISSP8-*Hind*IIIRev: TGTCAAGCTTTCAATCACTATCGCGCCTC

MISSP8-*Bgl*IIRev: TGTCAGATCTTCAATCACTATCGCGCCTC

Completed ihpRNA expression cassette was further cloned as a full length *Sac*I linearized pSILBAy plasmid into the T-DNA of the binary vector pHg to create pHg/pSγMiSSP8. The pHg/pSγMiSSP8 were used for transforming *L. bicolor* dikaryotic strain S238N with *Agrobacterium tumefaciens* strain AGL1 (Kemppainen and Pardo, 2010). The transformed fungal strains were selected with 300 μg.mL^{-1} hygromycin B (Invitrogen) and were later maintained under 150 μg.mL^{-1} hygromycin B selection pressure on modified P5 medium. Four randomly selected pHg/pSγMiSSP8 *L. bicolor* transformant strains were used for further molecular and physiological analyses.

Molecular analyses of Laccaria bicolor transformants

Plasmid rescue of the right border (RB) - linked gDNA was carried out with *Bam*HI cut and self-ligated *L. bicolor* gDNA according to Kemppainen et al. (2008). Sequencing of the rescued plasmids was done using M13/pUC-reverse primer (-26)17 mer. Left border (LB) TAIL-PCR was done according to Kemppainen et al., 2009, using T-DNA specific nested primers LB1.3 (Mullins et al., 2001) and arbitrary primer AD2 (Liu et al., 1995). L3/AD2 amplified TAIL-PCR products were TA-subcloned into pCR®2.1-TOPO® (Invitrogen) and sequenced with L3 primer. All the PCR reactions were carried out using T-personal thermocycler (Biometra ®) and PCR chemicals from Fermentas. Sequencing reactions were purchased from Macrogen Sequencing Service.

In vitro mycorrhization experiments

7

For *in vitro* mycorrhization tests between *P. tremula x P. alba* and *L. bicolor,* we used an existing "sandwich" co-culture system described in Felten et al. (2009). After three weeks of co-incubation of poplar cuttings with *L. bicolor*, at least 10 to 20 biological replicates were analysed for the percentage of colonized roots with the *L. bicolor* wild-type strain S238N or with the four *L. bicolor MiSSP8*-RNAi lines. Two independent empty vector transformants of *L. bicolor* (ev7 and ev9 lines, Plett et al, 2011) were also tested for their ability to colonize roots.

Motif analysis

For the identification of proteins sharing the DWRR motif found in MiSSP8 sequence, the following regular expression [DPSNAG]-W-[KR]-R-x(2,20) was scanned into 354 fungal proteomes available at the MycoCosm database (https://genome.jgi.doe.gov/programs/fungi/index.jsf), 2774 bacterial proteomes available at the NCBI website (ftp://ftp.ncbi.nlm.nih.gov/genomes/refseq/bacteria/) and 10 different plant proteomes available on the Phytozome website (https://phytozome.jgi.doe.gov/pz/portal.html) using the PS-Scan software (DeCastro et al, 2006). Only protein sequences starting with a methionine have been kept for further analysis. Protein sequences retrieved by PS-Scan were further analyzed by GLAM2 (Gapped Local Alignments Motifs) software v 4.11.0 (Frith et al., 2008) with default parameters in order to assess conservation of the DWRR motif. Similar GLAM2 analysis was performed also on shuffled sequences used as control.

Transient protein expression in Nicotiana benthamiana leaf cells

Agroinfiltration of 4 to 6 weeks-old *N. benthamiana* leaves with *A. tumefaciens* GV3101 was performed as described by Win et al. (2011). *A. tumefaciens* was transformed with the pK7FWG2.0 vector (Karimi et al., 2002) containing MiSSP8 (with or without its signal peptide) fused to eGFP or PCDB1 fused to mCherry. For co-transformation, *A. tumefaciens* strains were mixed in a 1:1 ratio in infiltration buffer (10 mM $MgCl_2$, 10 mM MES pH 5.6, 200 µM acetosyringone) to a final $O.D_{600}$ of 0.2. The leaves were collected two days after infiltration for microscopy analysis.

Callose Staining

8

Callose deposition at plasmodesmata was detected in leaf tissues infiltrated with 0.01 % (w/v) aniline blue (Sigma-Aldrich, USA) in 0.01 M K_3PO4 (pH 12), according to Zavaliev & Epel. (2015) and incubated in the dark for 1–2 hours before imaging.

Microscopy analysis of roots L. bicolor MiSSP8-mutant.

ECM root tips of *P. trichocarpa- L. bicolor* (WT or *MiSSP8*-RNAi lines) were fixed 24 h in 4% paraformaldehyde in PBS buffer (100 mM phosphate buffer, 2.7 mM KCl and 137 mM NaCl pH 7.4) at 4°C. The root segments were embedded in agarose 5% and cut into 25 µm radial sections with a Leica VT1200S Leica vibratome (Leica Microsystems). Sections were categorized according to their length (100, 200 and 600 µm) from the root apex. Sections were stained with wheat germ agglutinin (WGA)–Alexa Fluor® 633 Conjugate (W21404, ThermoFisher, France) and propidium iodide (Invitrogen, France). To compare the development of the Hartig net between samples, we ensured to take sections between 200 and 600 µm distance from the root apex.

Cell imaging by confocal laser-scanning microscopy

Living tobacco cells or transversal sections of ECM root tips were viewed either by a Zeiss LSM780 (Carl Zeiss AG, Germany) or a Leica TCS SP8 (Leica Microsystems, Germany) confocal laser scanning microscope system. Images were obtained with objectives CAPO-40x/1.2 water, PLNAPO-63x/1.4oil or PLAPOCS2-63x/12.30 oil-immersion objectives, acquired sequentially to exclude excitation and emission crosstalk (when required). The samples were observed at the excitation/emission wavelength of 405/437-491 nm, 488/514-521 nm and 592/597-618 for aniline blue, eGFP and mCherry, respectively. Images were processed with ZEN (Carl Zeiss AG) or LAS AF Lite (Leica Microsystem) softwares.

Quantitative RT-PCR

Expression of *MiSSP8* was assessed in free-living mycelium, colonized root tips and in fruiting bodies at different developmental stages. For the ectomycorrhizal root tips, extramatrical and free-living mycelium, real-time qPCR was performed in an optical 96-wells plate with a StepOne sequence detection system (Applied Biosystems, Life technologies) and fast cycling conditions (20 s at 95°C, 40 cycles of 3 s at 95°C and 30s at 60°C). Each 10 µl reaction contained 2X Fast SYBR green Master Mix (Applied Biosystems, life technologies),

9

300 nM gene-specific forward and reverse primer, water and 11 ng cDNA. Data were expressed relatively to the sample with the highest expression level ($2^{-(Ct-Ctmin)}$) and normalized against six reference genes (JGIv2 IDs #293350, #611151, #313997, #446085, #246915 and #319764). Stability of the reference genes was confirmed by geNorm analysis (Vandesompele et al., 2002). The normalisation factor NF for each sample was calculated as the geometric mean of the relative expression level of the six reference genes. Consequently, the expression level of *MiSSP8* for an individual sample was obtained by the formula $2^{-(Ct-Ctmin)}$/NF according to Vandesompele et al. 2002. Finally, data were rescaled relative to the FLM. For the fruiting bodies expression, cDNA were obtained from 500 ng of total RNAs using the i-Script cDNA reverse transcription kit (Biorad) in a final volume of 20 uL. RT-qPCR reactions were performed on 10 ng cDNA and 300 nM forward and reverse primer in each reaction, using the RotorGene (Qiagen) with the standard cycle conditions: 95 °C for 3 min; 40 cycles at 95 °C for 15 s and 65 °C for 30 s, followed by a melting curve analysis (temperature range from 65 °C to 95 °C with 0.5 °C increase every 10 s). Transcript abundance was normalized using *L. bicolor* histone H4 (JGIv2 ID# 319764) and ubiquitin (JGIv2 ID #446085)–encoding genes. Amplification efficiency (E) was experimentally measured for each primers pairs and was taken into account for calculation of normalized expression (Pfaffl et al., 2001).

Production of recombinant protein and biochemical analysis

MiSSP8Δ1-20 (*i.e.* devoid of its first twenty amino-acid residues) was synthesized by Genecust (Luxembourg) and subcloned into the pET-28a-CPDSalI vector (Shen et al., 2009) between *Nco*I and *Sal*I restriction sites. The resulting plasmids were subsequently used for the transformation of the Rosetta2 (DE3) pLysS strain of *E. coli* (Novagen). The expression of the recombinant proteins was performed at 37°C in Luria Bertani (LB) medium supplemented with 30 μg.ml^{-1} of kanamycin and 34 µg.ml^{-1} of chloramphenicol. When the cell culture reached an O.D$_{60}$0 of 0.7, recombinant protein expression was induced by the addition of 0.1 mM isopropyl β-D-1-thiogalactopyranoside (IPTG), and the cells were grown for a further 4 hours at 37°C. Cells were then harvested by centrifugation, resuspended in a 30 mM Tris/HCl pH 8.0, 200 mM NaCl lysis buffer and lysed by sonication. The cell extract was centrifuged at

10

35000 g for 25 min at 4°C to remove cellular debris and aggregated proteins. C-terminal His-tagged proteins were purified by gravity-flow chromatography on a nickel nitrilotriacetate (Ni-NTA) agarose resin (Qiagen) according to the manufacturer's recommendations followed by an exclusion chromatography on a Superdex75 column connected to an ÄKTA Purifier^{TM} (GE Healthcare). CPD-tag was cleaved using 200 µM inositol-6-phosphate as described by Schen et al. (2009), and removed by size exclusion chromatography. Isothermal calorimetry experiments were carried out at 20°C in 10 mM phosphate buffer with an ITC200 isothermal calorimeter (Malvern). The calorimetric cell was filled with an excess of laminarin hexamers (Megazyme), long chain laminarin (Invivogen), chitin hexamers (Elicityl) or chitosan hexamers (Elicityl) (4 < molar ratio < 40), first desalted using a PD10 desalting column (GE Healthcare) and resuspended in 10 mM phosphate buffer pH5 (except for chitosan which was resuspended in PBS buffer pH7). Circular dichroism experiments were carried out with 75 µM of recombinant MiSSP8 in 10 mM sodium phosphate buffer pH7 using a Chirascan Plus (Applied Photophysics).

Results

MiSSP8-encoding gene is up-regulated in ECM root tips and fruiting body.

Transcript profiling of *L. bicolor* free-living mycelium and *P. trichocarpa* colonized root tips have highlighted the presence of 98 Mycorrhiza-induced Small Secreted Proteins (MiSSPs) in this ECM fungus (Martin et al., 2008). Of these, *MiSSP8* displayed the third highest induction in mature ectomycorrhizal root tips (Martin et al., 2008). To determine the regulation of MiSSP8 throughout ECM development, we investigated *MiSSP8* expression during *in vitro* ECM time course with *P. tremula x alba* using real time-qPCR. At 7 days post-contact, fungal hyphae started colonization of fine roots and form the mantle. At 14 days, the Hartig net is present and at 21 days, fully mature ECM organ has developed. The low and constitutive-level of *MiSSP8* expression in free-living mycelium was set as a reference. *MiSSP8* was up-regulated in ECM root tips from day 7 to day 14, reaching its maximum induction at this latter time point (Fig. 1b). The expression decreased to reach the same level as in FLM at 21 days (mature ECM). Expression of *MiSSP8* in the extraradical mycelium (i.e, the part of the

11

rhizospheric mycelium not in contact with the roots) was the same as FLM all along the time course (Fig. 1b). In order to investigate the expression level of *MiSSP8* in a non-symbiotic tissue, we performed qRT-PCR on *L. bicolor* fruiting body tissues (stipe and cap) at two different developmental stages (early and late) (Fig. 1c, Fig. S2). The expression of *MiSSP8* in *L. bicolor* sporocarps is higher than its expression in FLM and ECM root tips. Overall, *MiSSP8* was strongly induced during fruiting body-development and *P. tremula x alba* root colonisation (mantle and Hartig net formation).

MiSSP8 is secreted as indicated by the yeast invertase secretion assay

MiSSP8 is a protein of 70 amino acids, the first twenty residues of which encode a predicted signal peptide as predicted by SignalP v4.1 (Fig. 1a). The mature MiSSP8 is composed of 50 amino acids, with a predicted molecular weight of 6105.32 Da and a theoretical pI of 5.12. According to the hydrophobicity plot, the mature MiSSP8 is a hydrophilic protein with charged amino acids exposed to solvent (Fig. 1a) but there is no predicted secondary structure (Fig. S1a). A circular dichroism experiment performed on the recombinant protein produced in *E. coli* further confirms the lack of secondary structure of MiSSP8 (Fig. S1b). This protein displayed sequence similarities with only one protein of *Laccaria amethystina* (JGIv2 #676588), a close relative of *L. bicolor*, according to BLASTP search NCBI and JGI MycoCosm databases. Altogether, these data suggest that MiSSP8 is a natively unstructured protein without sequence similarities with previously characterized proteins. In order to confirm that the predicted signal peptide is functional and properly processed, we fused the full length MiSSP8 (including its signal peptide) to the yeast invertase *SUC2*, catalysing the hydrolysis of sucrose. The transformed yeasts were able to grow on a minimal medium supplemented with sucrose and antimycin (Fig. 1d, bottom right) like the yeast transformed with a full-length invertase (Fig. 1d, bottom left). Yeasts transformed with an empty vector control (Fig. 1d, top left) or an invertase fused to MiSSP8 lacking its signal peptide (Fig. 1d, top right) did not grow on the same medium. These results demonstrate that the signal peptide of MiSSP8 was properly recognized and processed in yeast and that it triggered the secretion of the invertase. Therefore, it is likely that *L. bicolor* secretes MiSSP8 into the extracellular space during root colonization and fruiting body development.

12

MiSSP8 possess a repetitive motif shared with other fungal secreted proteins

At its C-terminus, MiSSP8 contains a 25 amino acids long sequence carrying a repetitive motif of one aspartate, one tryptophan and two arginines (i.e. DWRR). This motif is repeated four times in MiSSP8 and spaced with two amino-acids (Fig. 1a). It did not possess any match in motif databases such as PROSITE and PFAM. The *L. amethystina* protein sharing sequence similarities with MiSSP8 contains six repetitive motif spaced by more than two residues. The motif found in the *L. amethystina* protein was quite conserved albeit the first amino acid was different and the third amino acid can be either an arginine or a lysine. Moreover, a MCL (Markov Cluster Algorithm) analysis performed on a set of 49 genomes had previously retrieved 33 proteins containing a similar motif as MiSSP8, also with a variation on the first and the third amino acid of the motif (Kohler et al, 2015). Therefore, we designed the following pattern [DPSNAG]-W-[KR]-R-x(2,20) to take into account this variability. Using pattern search instead of sequence homology, we identified a total of 74 proteins from 39 different fungi containing this repetitive motif (Table S1). Using GLAM2, we were able to identify a new motif shared between these 39 fungi named DWRR/DWRR-like (Fig. 2a). Interestingly, whereas the search was performed on a total of 354 fungal proteomes available on the MycoCosm database, 2774 bacterial proteomes available on the NCBI database, 11 plant proteomes available in the Phytozome database (Table S2), the motif was only found in proteins from organisms belonging to the kingdom Fungi (Table S1). Thirty one of these fungi were saprotrophic (wood decayers, litter decayers, white rot or brown rot), five were ectomycorrhizal, one was a root pathogen, one was designed as a plant associated fungus and one had a yet undefined lifestyle (Table S1). The median size of the proteins detected was 144 amino acids, ranging from 70 to 738 (Fig. 2b), and most of them (64/74) contained a predicted signal peptide at their N-termini (Table 1). The number of motifs present in each protein sequences varied from 4 to 17 (Fig. 2c). No protein domains were detected by PFAM or PROSITE databases searches on these MiSSP8-like proteins, except for three proteins from the white rot fungus *Schizophyllum commune*, which possess a N-terminal aspartic peptidase A1 domain as confirmed by PSI-Search (Fig. 3, Supplementary File S1). RNA-Seq analysis performed on *Pinus pinaster* root tips colonized by the

13

ectomycorrhizal *Hebeloma cylindrosporum* showed that two of the three SSPs from *H. cylindrosporum* containing the DWRR or DWRR-like motif were up-regulated during the root colonization (Doré et al, 2015; GEO accession number GSE63868 and GSE66156 ; Supplementary Table S3). In conclusion, the repetitive motif DWRR is found in both *L. bicolor* MiSSP8 sequence and secreted proteins from wood decayers and ectomycorrhizal fungi. It suggests that MiSSP8 might have evolved from saprotrophic SSP ancestors.

RNAi-mediated knockdown of MiSSP8 encoding gene impairs mycorrhization rate

Since *MiSSP8* expression is induced during the early steps of ectomycorrhizal symbiosis development, we assessed whether MiSSP8 is required for establishment of symbiotic interaction. Generation of knockout mutants through homologous recombination has not been accomplished so far in *L. bicolor*. However, genetic tools to obtain *Laccaria* strains with significantly reduced target gene expression levels through RNA interference (RNAi) are available (Kemppainen et al., 2009; Kemppainen & Pardo 2010). RNAi hairpins targeting the MiSSP8 transcripts were expressed in *L. bicolor* through *A. tumefaciens* mediated transformation (ATMT). A transgenic ATMT *Laccaria* library was generated and 24 randomly selected independent RNAi lines were passed through consecutive hygromycin B selection steps. Among these, four *Laccaria* RNAi lines were analyzed at molecular level (Plett et al, 2011; Supplementary Table S4). Real-time qPCR analysis confirmed down-regulation of *MiSSP8* in the four transgenic lines, with a reduction from 82% to 95% compared to the empty-vector control lines (Fig. 4a). We quantified the ability of these transgenic RNAi lines to colonize *P. tremula x alba* roots *in vitro*. The mycorrhization rate, defined as percentage of ECM root tips formed over the total number of lateral roots, was found significantly reduced in the mutants, being 45% for the wild-type and empty-vector controls and only 10 to 15% for the four *L. bicolor MiSSP8*-RNAi lines (Fig. 4b). These results demonstrate that MiSSP8 is required for ECM symbiosis.

RNAi-mediated knockdown of *MiSSP8* impairs formation of fungal mantle and subsequent Hartig net development

To estimate whether MiSSP8 is necessary for fungal mantle and Hartig net development (two hallmarks of the mature ectomycorrhiza), we performed microscopy analysis on ECM root

14

tips formed. After one week of contact, the fungal mantle formed by *MiSSP8*-RNAi lines was strongly unstructured and thinner than the one obtained with the reference strain (empty vector control). After two weeks, *MiSSP8*-RNAi lines displayed one or two layers of fungal hyphae forming the mantle (Fig. 4c). This observation contrasts with the fungal mantle formed with the control transformant strain, which displayed a thick and well-organized fungal sheath with several layers of fungal hyphae stacked on each other. More strikingly, *MiSSP8*-RNAi lines were impaired in their ability to form the Hartig net even after 15 days of contact (Fig. 4c). As MiSSP8 is likely secreted by fungal hyphae, we investigated whether MiSSP8 would be able to bind to fungal cell wall-carbohydrates (β1-3 glucans, chitin and chitosan). In our conditions, recombinant MiSSP8 was not able to bind neither chitin, chitosan nor β1-3 glucans (Fig. S3a,b). Altogether, these findings highlight the involvement of MiSSP8 in the establishment of the ECM symbiosis. MiSSP8 is involved in the differentiation of the fungal mantle precluding hyphal expansion to form the Hartig net.

MiSSP8 co-localizes with plasmodesmata when expressed *in planta*.

Since MiSSP8 is likely secreted by fungal hyphae, we checked its subcellular localization *in planta*. Subcellular localization of MiSSP8Δ1-20::eGFP (i.e. MiSSP8 devoid of its signal-peptide) and MiSSP8::eGFP (MiSSP8 with its signal peptide) was performed in *N. benthamiana* epidermal cells. PDCB1::mCherry (i.e. PlasmoDesmata Callose Binding protein 1, Gene ID/TAIR: AT5G61130) was co-expressed as a marker for plasmodesmata. Cells expressing PDCB1::mCherry and MiSSP8::eGFP showed discrete punctate structures characteristic of plasmodesmata. Overlapping fluorescence intensity profiles of both detection channels indicate a co-localization of MiSSP8::eGFP and plasmodesmata (Fig. 5a). Notably, MiSSP8Δ1-20::eGFP localizes in cytosol and nucleus but not in plasmodesmata (Fig. 5b). This indicates that the localization of MiSSP8 in plasmodesmata requires its secretion. To ensure detection of a specific localization, instead of an artefact due to interaction between the two fusion proteins, we used aniline blue to stain callose within plasmodesmata in leaves expressing MiSSP8::eGFP. There is no strict co-localization between MiSSP8 and callose of plasmodesmata, but MiSSP8::eGFP signal is detected on either sides of the punctate callose localization (Fig. 5c). To check whether MiSSP8 is interacting with callose, we investigated

15

the ability of recombinant MiSSP8 to interact with laminarin, a structural analogue of callose, by isothermal calorimetry. In the condition tested, recombinant MiSSP8 was not able to bind laminarin (Fig. S3c,d). Our data indicate that MiSSP8 localizes in plasmodesmata without the capacity of callose-binding.

Discussion

MiSSP8: a small-secreted protein likely required for hyphal aggregation, important for both symbiotic and non-symbiotic processes

Several MiSSPs from *L. bicolor*, including MISSP8, are known to be part of the "core" regulon expressed during the colonization of two hosts, *Populus trichocarpa* and *Pseudotsuga menziesii* (Plett et al., 2015a). These proteins have hence been hypothesized to be key genes required for the symbiosis development in *L. bicolor* (Plett et al., 2015a). The strong decrease in the ability to form mycorrhizae for the *MiSSP8*-targeted RNAi lines is consistent with this hypothesis. In addition, we clearly show that MiSSP8 is directly involved in the symbiosis establishment, through a role played in mantle formation and the subsequent Hartig net development. This study is the second one describing *L. bicolor* MiSSP as a genetic determinant required for ECM symbiosis.

Real-time qPCR performed on the free-living mycelium, the symbiotic tissues and the fruiting body showed a high level of *MiSSP8* expression both in the mycorrhizal root tips and the fruiting body but not in the free-living mycelium. This expression profile suggests an involvement of MiSSP8 in both symbiosis-related (i.e. formation of ectomycorrhiza) and non-symbiosis-related processes (i.e. fruiting body formation). Both the ectomycorrhizal mantle sheath and the fruiting body tissues are composed of pseudoparenchyma, a pseudo-tissue made of aggregated hyphae that looks similar to the plant parenchyma (Peterson & Farquhar, 1994; Brunner & Scheidegger, 1992). Ectomycorrhiza developed by *MiSSP8*-RNAi lines display a disorganized fungal mantle and no Hartig net formation. This phenotype could be the results of the lack of fungal aggregation. Hyphae from mantle are indeed glued together and embedded in an extracellular material composed of glycoproteins and fungal polysaccharides (e.g. chitin, β 1-3 glucans) (Massicotte et al., 1990; Dexheimer et al., 1994).

16

Previous studies propose a sequential role of small-secreted proteins, namely hydrophobins and polypeptides with a RGD motif (e.g. SRAP32), in the aggregation of hyphae during mantle development in the ectomycorrhizal fungi *Pisolithus tinctorius* (reviewed in Martin et al., 1999). We also notice that MiSSP8 is a hydrophilic protein with charged amino-acids exposed to solvent, but was not able to bind chitin, chitosan nor β1-3 glucans (i.e. laminarin) in our conditions. This suggests that MiSSP8 is likely not anchored in fungal cell walls.

Therefore, we suggest that MiSSP8, a hydrophilic small-secreted protein, participates in pseudoparenchyma formation by aggregating fungal hyphae. Hence, hyphal aggregation would be required to achieve both symbiotic and non symbiotic-related functions, in line with the concept that the ECM fungi have adapted some of their saprotrophic capacities to the interaction with their host plant (Doré et al., 2015).

Identification of a novel fungal-specific motif highly represented in the proteomes of saprotrophic fungi

As MiSSP8 displays sequence similarities with only one *L. amethystina* protein, we conclude that MiSSP8 is a *Laccaria*-specific gene up-regulated both in symbiosis and in fruiting bodies. These lineage-specific genes may have been formed *de novo*, derived from neofunctionalization of duplicated genes or from ancestral genes that have strongly diverged due to selection pressure (Kohler et al., 2015). However, despite the absence of sequence similarities, we identify a novel repetitive motif $(DWRR)_n$ at the C-terminus of MiSSP8. This repetitive motif seems restricted to fungi as no such protein motif was identified in the bacterial or plant proteomes analysed. Fungal MiSSP8-like proteins identified in our study exhibit the $(DWRR)_n$ motif at their C-termini with a variable number of repetitions, but these fungal proteins did not share sequence similarities at their N-termini. Based on their difference of size and sequence, the function carried out by these proteins is likely to be different and these proteins might be involved in various cellular functions. The fungal specific CFEM (Common in several Fungal Extracellular Membrane proteins) domain is also associated with proteins involved in different biological activities (Kulkami et al., 2003; Zhang et al., 2015) e.g. cell wall stability (Vaknin et al., 2014), biofilm formation (Pérez et

17

al., 2006) or iron homeostasis (Srivastava et al., 2014). Comparative phylogenomics of 49 fungal genomes revealed that ECM fungi have evolved several times from saprotrophic ancestors, either white rot, brown rot or soil decayers, by developing a set of symbiotic genes with rapid turn-over (Kohler et al., 2015). Consistently with this finding, *MiSSP8* is a *Laccaria*-specific gene containing a fungal specific repetitive motif that might have been inherited from proteins from saprotrophic ancestors. Since MiSSP8 is likely playing a role in the formation of the pseudoparenchyma of both non-symbiotic (sporocarps) and symbiotic (ECM) structures, we propose that MiSSP8 function, initially required for *L. bicolor* fruiting body formation, has been recruited for the establishment of the symbiosis. In-depth functional analysis of MiSSP8 and its saprotrophic related SSPs will be necessary to (i) clarify whether these proteins fulfil similar function or not, and (ii) study whether the $(DWRR)_n$ motif is required for MiSSP8 function.

Identification of fungal proteins predicted as secreted and containing a repetitive motif similar to the one of MiSSP8 raises the question of the role of this repetitive pattern. The most conserved part of this motif, WR/KR, is similar to the Kexin endoproteinase cleavage site RR or WR (Mizuno et al., 1988; Mizuno et al., 1989). Cleavage of proteins by a Kex2-like protease has been shown to be required for the virulence of several pathogenic fungi (Jacob-Wilk et al., 2009 ; Teertstra et al., 2006 ; Moyes et al., 2016). Therefore, the proteins containing the $(DWRR)_n$ motif could be processed prior to or after their secretion in order to become active. Looking for the presence of such peptides during symbiotic life phase of *Laccaria* will be of particular interest.

MiSSP8 co-localizes with plasmodesmata in *N. benthamiana* leaves

In this study, we demonstrate that the signal-peptide of MiSSP8 is correctly processed in a heterologous yeast system. Together with *MiSSP8* up-regulation in ECM, our results strongly suggest that *Laccaria* secretes this protein during ectomycorrhiza formation. Using agroinfiltration assays, we show that MiSSP8 (with its signal-peptide) co-localizes with PDCB1, a callose-binding plant protein used as a marker for plasmodesmata (PD). Co-localization of MiSSP8 with PDs is likely not due to a direct interaction between MiSSP8 and callose as shown by ITC experiments and by partial colocalization between callose and

18

MiSSP8. However, this localization was obtained using expression of MiSSP8::eGFP in tobacco leaves, an heterologous system, and should be confirmed in the host cells. PDs connect the cytoplasm, the endoplasmic reticulum (named desmotubule) and the plasma membrane of neighbouring living cells by traversing the plant cell walls. Reversible deposition of callose in the cell wall at the plasmodesmata neck region controls size of the plasmodesmal pore and consequently cell-to-cell communication (for review, see Lee and Lu, 2011; Tilsner et al., 2016). Whether the cortical symplast breaks up or is conserved during fungal colonization to form the Hartig net is debated. Nylund (1980) found PD in TEM sections of both *in vitro* and natural ectomycorrhiza formed between Norway spruce (*Picea abies*) and *Piloderma bicolor*. However, numerous studies highlight the destruction of plasmodesmata connections (i.e lack of symplastic continuity) in cortical cells surrounded by fungal hyphae forming the Hartig net (Peterson and Bonfante, 1994; Piché et al., 1983). A lost of PD when the Hartig net is present would imply that nutrients must pass to the apoplastic interface before they can be absorbed either by fungal or plant cells. Plasmodesmata do not only provide a direct cell-to-cell route for small soluble molecules, such as metabolites, sugars and hormones, but they also provide a way of transport for proteins and RNA. Interestingly, several recent studies have highlighted the fact that effectors of plant pathogens (virus and fungi) migrate between cells via PD (Cheval and Faulkner, 2017; Benitez-Alfonso et al., 2010; Kankanala et al., 2007). Furthermore, proteomics data indicate the presence of receptor-like kinase, responsible for recognition of MAMP (Microbe-Associated Molecular Pattern), specifically at PD (Faulkner, 2013; Lee, 2015). Several authors thus propose a novel role for PDs as a signalling hub whose control is required for influencing the outcome of plant-pathogen interactions. Our data suggest that PDs could also be crucial for mutualistic plant-fungus interaction to occur. However, further studies are needed to better understand and demonstrate the role of symplastic connectivity in both the development and the functioning of ectomycorrhizal symbiosis.

In conclusion, we characterized the Mycorrhiza induced Small Secreted Protein of 8 kDa (MiSSP8) by combining functional and *in silico* approaches. We demonstrate that MiSSP8

19

has a functional secretion signal peptide and that this protein is a decisive factor for symbiosis establishment. *MiSSP8*-mutants are impaired in ectomycorrhizal mantle formation, precluding the subsequent Hartig net formation. Moreover, *MiSSP8* is up-regulated in sporocarps. MiSSP8 contains a novel motif prevalent in SSP from saprotrophic and ectomycorrhizal fungi. Our data suggest that MiSSP8 is a small-secreted protein with a possible dual role: one in basic fungal biology regulating hyphal aggregation and another *in planta*, related to its plasmodesmata co-localization.

Acknowledgments

Authors contributions

CVF, FM designed and managed the project; CP, YD, FG, MK, JR, MBP, AH, CVF performed the experiments; CP, CVF, AP, HG analyzed the data; CP, EM performed the bioinformatic analysis; CP, CVF, FM wrote the manuscript and all authors revised it.

References

20

1. **Akum, F. N., Steinbrenner, J., Biedenkopf, D., Imani, J., and Kogel, K.-H. 2015**. The *Piriformospora indica* effector PIIN_08944 promotes the mutualistic Sebacinalean symbiosis. *Front. Plant Sci*. 6:906

2. **Balestrini, R., and Kottke, I. 2016**. Structure and development of ectomycorrhizal roots. Pages 47–61 in:Molecular Mycorrhizal Symbiosis,

3. **Benitez-Alfonso, Y., Faulkner, C., Ritzenthaler, C., and Maule, A. J. 2010**. Plasmodesmata: Gateways to Local and Systemic Virus Infection. *Mol. Plant-Microbe Interact*. 23:1403–1412

4. **Berg, G., Mahnert, A., and Moissl-Eichinger, C. 2014**. Beneficial effects of plant-associated microbes on indoor microbiomes and human health? *Front. Microbiol*. 5

5. **Berg, S., Pimenov, A., Palmer, C., Emmerson, M., and Jonsson, T**. **2015**. Ecological communities are vulnerable to realistic extinction sequences. *Oikos*. 124:486–496

6. **Brundrett, M. C. 2009**. Mycorrhizal associations and other means of nutrition of vascular plants: Understanding the global diversity of host plants by resolving conflicting information and developing reliable means of diagnosis. *Plant Soil.* 320:37–77

7. **Brunner, I., and Scheidegger, C. 1992**. Ontogeny of synthesized Picea abies (L.) Karst.–Hebeloma crustuliniforme (Bull. ex St Amans) Quél. ectomycorrhizas. *New Phytol.* 120:359–369

8. **Buée, M., Reich, M., Murat, C., Morin, E., Nilsson, R. H., Uroz, S., and Martin, F. 2009**. 454 Pyrosequencing analyses of forest soils reveal an unexpectedly high fungal diversity. *New Phytol*. 184:449–456

9. **Cheval, C., and Faulkner, C. 2017**. Plasmodesmal regulation during plant-pathogen interactions. *New Phytol.* :1–6

10. **de Castro, E., Sigrist, C. J. A., Gattiker, A., Bulliard, V., Langendijk-Genevaux, P. S., Gasteiger, E., Bairoch, A., and Hulo, N. 2006**. ScanProsite: Detection of PROSITE signature matches and ProRule-associated functional and structural residues in proteins. *Nucleic Acids Res*. 34

11. **Dexheimer, J., Gerard, J., and Genet, P. 1994**. Study of transformations of the root system of *Eucalyptus globulus* associated with *Pisolithus tinctorius*. I. Aptitude to mycorrhization of different kinds of roots. *Phytomorphology*. 44:235–245

12. **Ditengou, F. A., Müller, A., Rosenkranz, M., Felten, J., Lasok, H., van Doorn, M. M., Legué, V., Palme, K., Schnitzler, J.-P., and Polle, A. 2015**. Volatile signalling by sesquiterpenes from ectomycorrhizal fungi reprogrammes root architecture. Nat. Commun. 6:6279

13. **Doré, J., Perraud, M., Dieryckx, C., Kohler, A., Morin, E., Henrissat, B., Lindquist, E., Zimmermann, S. D., Girard, V., Kuo, A.,** *et al.* **2015**. Comparative genomics, proteomics and transcriptomics give new insight into the exoproteome of the basidiomycete *Hebeloma cylindrosporum* and its involvement in ectomycorrhizal symbiosis. *New Phytol.* 208:1169–1187

14. **Drozdetskiy A, Cole C, Procter J, Barton GJ. 2015**. JPred4: a protein secondary structure prediction server. Nucleic Acids Research 43: W389–W394.

15. **Faulkner, C., Petutschnig, E., Benitez-Alfonso, Y., Beck, M., Robatzek, S., Lipka, V., and Maule, A. J. 2013**. LYM2-dependent chitin perception limits molecular flux via plasmodesmata. *Proc. Natl. Acad. Sci*. 110:9166–9170

16. **Felten, J., Kohler, A., Morin, E., Bhalerao, R. P., Palme, K., Martin, F., Ditengou, F. A., and Legue, V. 2009**. The Ectomycorrhizal Fungus *Laccaria bicolor* Stimulates Lateral Root Formation in Poplar and Arabidopsis through Auxin Transport and Signaling. *Plant Physiol.* 151:1991–2005

17. **Fierer, N., Breitbart, M., Nulton, J., Salamon, P., Lozupone, C., Jones, R., Robeson, M., Edwards, R. A., Felts, B., Rayhawk *et al.* 2007**. Metagenomic and small-subunit rRNA analyses reveal the genetic diversity of bacteria, archaea, fungi, and viruses in soil. *Appl. Environ. Microbiol*. 73:7059–7066

18. **Frith, M. C., Saunders, N. F. W., Kobe, B., and Bailey, T. L. 2008**. Discovering sequence motifs with arbitrary insertions and deletions. *PLoS Comput. Biol*. 4

19. **Genre, A., and Bonfante, P. 2012**. The Interface Between Plants and Mycorrhizal Fungi: Nutrient Exchange, Signaling and Cell Organization. Pages 39–49in:*The Mycota, IX: Fungal Associations 2nd* Ed,B. Hock, ed.Springer Berlin Heidelberg, Berlin, Heidelberg.

20. **Gietz, R. D., and Schiestl, R. H. 2008**. High-efficiency yeast transformation using the LiAc / SS carrier DNA / PEG method. *Nat. Protoc*. 2:31–35

21. **Jacob-Wilk, D., Turina, M., Kazmierczak, P., and Van Alfen, N. K. 2009**. Silencing of Kex2 Significantly Diminishes the Virulence of *Cryphonectria parasitica*. *Mol. Plant-Microbe Interact*. 22:211–221

22. **Jacobs, K. A., Collins-Racie, L. A., Colbert, M., Duckett, M., Golden-Fleet, M., Kelleher, K., Kriz, R., La Vallie, E. R., Merberg, D., Spaulding, V. et al. 1997**. A genetic selection for isolating cDNAs encoding secreted proteins. *Gene*. 198:289–296

23. **Kankanala, P., Czymmek, K., and Valent, B. 2007**. Roles for Rice Membrane Dynamics and Plasmodesmata during Biotrophic Invasion by the Blast Fungus. *Plant Cell.* 19:706–724

24. **Karimi, M., Inzé, D., and Depicker, A. 2002**. GATEWAY[TM] vectors for *Agrobacterium*-mediated plant transformation. *Trends Plant Sci*. 7:193–195

25. **Kemppainen, M. J., and Pardo, A. G.** 2010. pHg/pSILBAγ vector system for efficient gene silencing in homobasidiomycetes: Optimization of ihpRNA - Triggering in the mycorrhizal fungus *Laccaria bicolor*. *Microb. Biotechnol*. 3:178–200

26. **Kemppainen, M., Circosta, A., Tagu, D., Martin, F., and Pardo, A. G. 2005**. Agrobacterium-mediated transformation of the ectomycorrhizal symbiont *Laccaria bicolor* S238N. *Mycorrhiza*. 16:19–22

27. **Kemppainen, M., Duplessis, S., Martin, F., and Pardo, A. G. 2008.** T-DNA insertion, plasmid rescue and integration analysis in the model mycorrhizal fungus *Laccaria bicolor*. *Microb. Biotechnol*. 1:258–269

28. **Kemppainen, M., Duplessis, S., Martin, F., and Pardo, A. G. 2009**. RNA silencing in the model mycorrhizal fungus *Laccaria bicolor*: Gene knock-down of nitrate reductase results in inhibition of symbiosis with *Populus. Environ. Microbiol*. 11:1878–1896

22

29. **Kloppholz, S., Kuhn, H., and Requena, N. 2011**. A secreted fungal effector of *Glomus intraradices* promotes symbiotic biotrophy. *Curr. Biol*. 21:1204–1209

30. **Kohler, A., Kuo, A., Nagy, L. G., Morin, E., Barry, K. W., Buscot, F., Canbäck, B., Choi, C., Cichocki, N., Clum, A., et al. 2015**. Convergent losses of decay mechanisms and rapid turnover of symbiosis genes in mycorrhizal mutualists. *Nat. Genet.* 47:410–415

31. **Krause, K., Henke, C., Asiimwe, T., Ulbricht, A., Klemmer, S., Schachtschabel, D., Boland, W., and Kothe, E. 2015**. Biosynthesis and secretion of indole-3-acetic acid and its morphological effects on Tricholoma vaccinum-spruce ectomycorrhiza. Appl. Environ. Microbiol. 81:7003–7011

32. **Kulkarni, R. D., Kelkar, H. S., and Dean, R. A. 2003**. An eight-cysteine-containing CFEM domain unique to a group of fungal membrane proteins. *Trends Biochem. Sci*. 28:118–121

33. **Lakkireddy, K., Navarro-González, M., Velagapudi, R., and Kües, U. 2011.** Proteins expressed during hyphal aggregation for fruiting body formation in basidiomycetes. in: Proceedings of the 7th International Conference on Mushroom Biology and Mushroom Products,

34. **Lagrange, H., Jay-Allgmand, C., and Lapeyrie, F. 2001**. Rutin, the phenolglycoside from eucalyptus root exudates, stimulates Pisolithus hyphal growth at picomolar concentrations. New Phytol. 149:349–355

35. **Lee, J. Y. 2015**. Plasmodesmata: A signaling hub at the cellular boundary. *Curr. Opin. Plant Biol.* 27:133–140

36. **Lee, J. Y., and Lu, H. 2011**. Plasmodesmata: The battleground against intruders. *Trends Plant Sci.* 16:201–210

37. **Lindahl, B. D., and Tunlid, A. 2015**. Ectomycorrhizal fungi - potential organic matter decomposers, yet not saprotrophs. *New Phytol.* 205:1443–1447

38. **Liu, Y., Guang, G., Mitsukawa, N., Oosumi, T., and Whittier, R. F. 1995**. Efficient isolation and mapping of *Arabidopsis thaliana* T-DNA insert junctions by thermal asymmetric interlaced PCR. *Plant J.* 8:457–463

39. **Lo Presti, L., Lanver, D., Schweizer, G., Tanaka, S., Liang, L., Tollot, M., Zuccaro, A., Reissmann, S., and Kahmann, R. 2015**. Fungal Effectors and Plant Susceptibility. *Annu. Rev. Plant Biol.* 66:513–545

40. **Martin, F., Aerts, A., Ahrén, D., Brun, A., Danchin, E. G. J., Duchaussoy, F., Gibon, J., Kohler, A., Lindquist, E., Pereda *et al.* 2008**. The genome of *Laccaria bicolor* provides insights into mycorrhizal symbiosis. Nature. 452:88–92

41. **Martin, F., Kohler, A., Murat, C., Veneault-Fourrey, C., and Hibbett, D. S. 2016**. Unearthing the roots of ectomycorrhizal symbioses. *Nat. Rev. Microbiol.* 14:760–773

42. **Martin, F., Laurent, P., de Carvalho, D., Voiblet, C., Balestrini, R., Bonfante, P., and Tagu, D. 1999**. Cell wall proteins of the ectomycorrhizal basidiomycete *Pisolithus tinctorius*: identification, function, and expression in symbiosis. *Fungal Genet. Biol.* 27:161–174

43. **Massicotte, H. B., Peterson, R. L., Ackerley, C. A., and Melville, L. H. 1990.** Structure and ontogeny of *Betula alleghaniensis – Pisolithus tinctorius* ectomycorrhizae. *Can. J. Bot*. 68:579–593

44. **Mizuno, K., Nakamura, T., Ohshima, T., Tanaka, S., and Matsuo, H. 1988**. Yeast KEX2 gene encodes an endopeptidase homologous to subtilisin-like serine proteases. *Biochem. Biophys. Res. Commun*. 156:246–254

45. **Mizuno, K., Nakamura, T., Ohshima, T., Tanaka, S., and Matsuo, H. 1989.** Characterization of KEX2-encoded endopeptidase from yeast *Saccharomyces*, cerevisiae. Biochem. Biophys. *Res. Commun*. 159:305–311

46. **Moyes, D. L., Wilson, D., Richardson, J. P., Mogavero, S., Tang, S. X., Wernecke, J., Höfs, S., Gratacap, R. L., Robbins, J., Runglall, M. *et al.* 2016**. Candidalysin is a fungal peptide toxin critical for mucosal infection. *Nature*. 532:64–68

47. **Mullins, E. D., Chen, X., Romaine, P., Raina, R., Geiser, D. M., and Kang, S. 2001**. *Agrobacterium*-Mediated Transformation of *Fusarium oxysporum*: An Efficient Tool for Insertional Mutagenesis and Gene Transfer. *Phytopathology*. 91:173–180

48. **Murashige, T., and Skoog, F. 1962**. A Revised Medium for Rapid Growth and Bio Assays with Tobacco Tissue Cultures. *Physiol. Plant.* 15:473–497

49. **Nylund, J. ☐E. 1980**. Symplastic continuity during hartig net formation in norway spruce ectomycorrhizae. *New Phytol*. 86:373–378

50. **Paschlewski, and Paschlewskia**. **1974**. Studies on symbiotic properties of mycorrhizal fungi of pine (*Pinus sylvestris* L.) with the aid of the method of mycorrhizal synthesis in pure culture on agar. (Translated into English by Royal Dzieciolowski). Warsaw, Pol. For. Res. Inst.

51. **Pellegrin, C., Morin, E., Martin, F. M., and Veneault-Fourrey, C. 2015**. Comparative analysis of secretomes from ectomycorrhizal fungi with an emphasis on small-secreted proteins. *Front. Microbiol*. 6

52. **Pérez, A., Pedrós, B., Murgui, A., Casanova, M., López-Ribot, J. L., and Martínez, J. P. 2006**. Biofilm formation by *Candida albicans* mutants for genes coding fungal proteins exhibiting the eight-cysteine-containing CFEM domain. *FEMS Yeast Research*. 1074–1084

53. **Peterson, A. R. L., and Farquhar, M. L. 1994.** Mycorrhizas : Integrated Development between Roots and Fungi. *Mycologia*. 86:311–326

54. **Pfaffl, M. W. 2001**. A new mathematical model for relative quantification in real-time RT-PCR. *Nucleic Acids Res.* 29:45e–45

55. **Piché, Y., Peterson, R. L., Howarth, M. J., and Fortin, J. A. 1983.** A structural study of the interaction between the ectomycorrhizal fungus *Pisolithus tinctorius* and *Pinus strobus* roots. *Can. J. Bot.* 61:1185–1193

56. **Plett, J. M., and Martin, F. 2015**. Reconsidering mutualistic plant-fungal interactions through the lens of effector biology. *Curr. Opin. Plant Biol.* 26:45–50

57. **Plett, J. M., Daguerre, Y., Wittulsky, S., Vayssieres, A., Deveau, A., Melton, S. J., Kohler, A., Morrell-Falvey, J. L., Brun, A., Veneault-Fourrey, C. *et al.* 2014**. Effector MiSSP7 of the mutualistic fungus *Laccaria bicolor* stabilizes the *Populus*

JAZ6 protein and represses jasmonic acid (JA) responsive genes. *Proc. Natl. Acad. Sci.* 111:8299–8304

58. **Plett, J. M., Kemppainen, M., Kale, S. D., Kohler, A., Legué, V., Brun, A., Tyler, B. M., Pardo, A. G., and Martin, F. 2011**. A secreted effector protein of *Laccaria bicol*or is required for symbiosis development. *Curr. Biol.* 21:1197–1203

59. **Plett, J. M., Tisserant, E., Brun, A., Morin, E., Grigoriev, I. V., Kuo, A., Martin, F., and Kohler, A. 2015**. The Mutualist *Laccaria bicolor* Expresses a Core Gene Regulon During the Colonization of Diverse Host Plants and a Variable Regulon to Counteract Host-Specific Defenses. *Mol. Plant-Microbe Interact.* 28:261–273

60. **Rineau F, Lmalem H, Ahren D, Shah F, Johansson T, Coninx L, Ruytinx J, Nguyen H, Grigoriev I, Kuo A *et al.* 2017**. Comparative genomics and expression levels of hydrophobins from eight mycorrhizal genomes. *Mycorrhiza*. 27:383–396

61. **Shen, A., Lupardus, P. J., Morell, M., Ponder, E. L., Sadaghiani, A. M., Garcia, K. C., and Bogyo, M. 2009**. Simplified, enhanced protein purification using an inducible, autoprocessing enzyme tag. *PLoS One*. 4

62. **Srivastava, V. K., Suneetha, K. J., and Kaur, R. 2014**. A systematic analysis reveals an essential role for high-affinity iron uptake system, haemolysin and CFEM domain-containing protein in iron homoeostasis and virulence in *Candida glabrata*. *Biochem. J.* 463:103–114

63. **Teertstra, W. R., Deelstra, H. J., Vranes, M., Bohlmann, R., Kahmann, R., Kämper, J., and Wösten, H. A. B. 2006**. Repellents have functionally replaced hydrophobins in mediating attachment to a hydrophobic surface and in formation of hydrophobic aerial hyphae in *Ustilago maydis*. *Microbiology*. 152:3607–3612

64. **Tilsner, J., Nicolas, W., Rosado, A., and Bayer, E. M. 2016**. Staying Tight: Plasmodesmal Membrane Contact Sites and the Control of Cell-to-Cell Connectivity in Plants. *Annu. Rev. Plant Biol.* 67:337–364

65. **Uroz, S., Buée, M., Murat, C., Frey-Klett, P., and Martin, F. 2010**. Pyrosequencing reveals a contrasted bacterial diversity between oak rhizosphere and surrounding soil. *Environ. Microbiol. Rep.* 2:281–288

66. **Vaknin, Y., Shadkchan, Y., Levdansky, E., Morozov, M., Romano, J., and Osherov, N. 2014**. The three *Aspergillus fumigatus* CFEM-domain GPI-anchored proteins (CfmA-C) affect cell-wall stability but do not play a role in fungal virulence. *Fungal Genet. Biol.* 63:55–64

67. **van Der Heijden, M. G. A., Klironomos, J. N., and Ursic, M. 1998**. Mycorrhizal fungal diversity determines plant biodiversity, ecosystem variability and productivity. *Nature*. 396:69–72

68. **Vandesompele, J., De Preter, K., Pattyn, ilip, Poppe, B., Van Roy, N., De Paepe, A., and Speleman, rank. 2002**. Accurate normalization of real-time quantitative RT-PCR data by geometric averaging of multiple internal control genes. *Genome Biol.* 3:34–1

69. **Vayssières, A., Pěnčík, A., Felten, J., Kohler, A., Ljung, K., Martin, F., and Legué, V. 2015.** Development of the Poplar -Laccaria bicolor Ectomycorrhiza

Modifies Root Auxin Metabolism, Signaling, and Response. Plant Physiol. 169:890–902

70. **Wawra, S., Fesel, P., Widmer, H., Timm, M., Seibel, J., Leson, L., Kesseler, L., Nostadt, R., Hilbert, M., Langen, G.** *et al.* **2016**. The fungal-specific β-glucan-binding lectin FGB1 alters cell-wall composition and suppresses glucan-triggered immunity in plants. *Nat. Commun.* 7:13188

71. **Win, J., Kamoun, S., and Jones,** A. M. E. **2011**. Purification of effector-target protein complexes via transient expression in *Nicotiana benthamiana. Methods Mol. Biol.* 712:181–194

72. **Zavaliev, R., and Epel, B. L. 2015**. Imaging Callose at Plasmodesmata Using Aniline Blue: Quantitative Confocal Microscopy. *Methods Mol. Biol.* 1217:105–119

73. **Zhang, Z.-N., Wu, Q.-Y., Zhang, G.-Z., Zhu, Y.-Y., Murphy, R. W., Liu, Z., and Zou, C.-G. 2015**. Systematic analyses reveal uniqueness and origin of the CFEM domain in fungi. *Sci. Rep.* 5:13032

Legends of Figures

Figure 1: **MiSSP8 is a secreted repeat-containing protein highly expressed in ectomycorrhizal root tips and stipe and cap tissues of the fruiting body.**

(a) Domain organization of MiSSP8 and its hydrophobicity score as obtained by Protscale software (Gasteiger et al, 2005) and the amino-acid scale from Kyle & Doolittle (1982) with a window size of 5.

(b) Real-time qPCR time course performed on *L. bicolor* extraradical mycelium (ExM), free-living mycelium (FLM) and during development of *Populus tremula* x *alba* ECM root tips. Expression of *MiSSP8* in FLM was set as a reference.

(c) Real-time qPCR analysis on the expression of *MiSSP8* in the fruiting body of *L. bicolor*, the cap and stipe, at both early and late stages of development. Stars indicate significant differences (pvalue < 0.05).

(d) Yeast signal trap assay shows that the signal peptide predicted in MiSSP8 sequence is functional in yeast. *Saccharomyces cerevisiae* was transformed either with empty vector control (top left), mature MiSSP8 (lacking its signal peptide) fused to mature invertase (MiSSP8Δ1-20::Invertase, top right), full-length invertase (with its signal peptide, bottom left) or full length MiSSP8 fused to mature invertase (MiSSP8::Invertase, bottom right).

Figure 2: MiSSP8 contains a novel repetitive motif found in proteins from saprotrophic and ectomycorrhizal fungi.

(a) DWRR/DWRR-like motif found in the MiSSP8 sequence is detected among several fungal proteins predicted as secreted. Conserved motif inferred from the analysis of the 74 protein sequences identified using the GLAM2 software.

(b) Size distribution (in amino acids) of the 74 DWRR/DWRR-like containing proteins within the different fungal lifestyles identified.

(c) Number of repetitions found in the 74 fungal proteins carrying the DWRR/DWRR-like motif.

27

Figure 3: The DWRR motif associates MiSSP8 with proteins from saprotrophic and ECM fungi. The modular structure of the proteins is shown. Protein domains identified by PROSITE and signal peptides predicted by SignalP v4.1 are annotated. Fungal species not yet characterized as white rot or brown rot are sorted as wood decayers.

Figure 4: Knockdown of *MiSSP8* impairs the establishment of ectomycorrhizal symbiosis.

(a) Expression was measured by qRT-PCR. All values are shown as mean ± standard deviation; n = 3. Stars indicate that expression is statistically different than control line based on t-test and a p value < 0.05. ev indicates fungal lines transformed with an empty vector (i.e. negative control).

(b) Knockdown of *MiSSP8* strongly decreases the number of ectomycorrhizal root tips compared to the wild-type strain or the empty vector controls. Percentage of mycorrhizal root tips formed by wild-type *L. bicolor* S238N and two empty vector transformation controls (ev7 and 9) versus four independent *L. bicolor MiSSP8*-RNAi lines. All values are shown as mean ± standard deviation; n=25; Stars indicate significant difference from wild-type, ev7 and ev9 using t-test and a p-value < 0.05.

(c) Transversal section of ectomycorrhizal root tips formed by ev7 control transformant line and *MiSSP8*-RNAi lines. The *MiSSP8*-RNAi lines displays a loose mantle and no Hartig net compared to the empty vector control strain (ev7). Scale bars: 10 m. Propidium iodide stains plant cell walls and nuclei (red) and WGA-Alexa488 stains fungal cell walls (green).

Figure 5: MISSP8::eGFP co-localizes with plasmodesmata in *Nicotiana benthamiana* leaves.

(a-b) *N. benthamiana* leaves were agro-infiltrated with a construct expressing PDCB1::mCherry, a marker for plasmodesmata, and either a construct expressing MiSSP8::GFP (MiSSP8 containing its predicted signal peptide) **(a)**, or MiSSP8Δ1-20::eGFP (mature form of MiSSP8) **(b)**. The fluorescence intensity profile across the arrow for both green and red channels is shown in the graph.

28

(c) Leaves expressing MiSSP8::eGFP were infiltrated with aniline blue to visualize callose of plasmodesmata. The fluorescence intensity profile across the arrow for both green and blue channels is shown in the graph. Scale bars indicate 10 μm.

Supplementary Figure S1: *In silico* **prediction and experimental validation of MiSSP8 secondary structure**. **(a)** Secondary structure of MiSSP8 as predicted by the JPred 4 server (Drozdetskiy et al, 2015). **(b)** Analysis of recombinant MiSSP8 secondary structure by circular dichroism.

Supplementary Figure S2: Fruiting body of *L. bicolor* at two different developmental stages. The cap and stipe of fruiting bodies from *L. bicolor* were harvested at early and late developmental stages in order to study the expression of *MiSSP8* during the development of the fruiting body.

Supplementary Figure S3: MiSSP8 is not able to bind neither laminarin (β1-3 glucans with β1-6 branching), chitin nor chitosan. Binding properties of recombinant protein MiSSP8 to hexamers **(a)** or long-chain **(b)** of laminarin **(c)** chitin hexamers or **(d)** chitosan hexamers to callose, chitin hexamers and chitosan hexamers were assessed by isothermal calorimetry experiments.

Supplementary Table S1: Proteins sharing the DWRR/DWRR-like motif. Protein sequences containing from two to twenty repetitions of the DWRR/DWRR-like motif in a set of 354 fungal proteomes, 2774 bacterial proteomes, 11 plants proteomes.

Supplementary Table S2: List of fungal, bacterial, plant and algae proteomes scanned. Set of 354 fungal proteomes available on the MycoCosm database, 2774 bacterial proteomes available on the NCBI database, 11 plants proteomes available on the Phytozome database, used to search for proteins containing the DWRR/DWRR-like motif.

Supplementary Table S3: RNA-Seq analysis of *Hebeloma cylindrosporum* in contact with *Pinus pinaster* root tips. Expression of the three proteins containing the DWRR motif in ectomycorrhizal root tips of *Pinus pinaster* colonized by *Hebeloma cylindrosporum.* Expression given in Read Per Kilobases of transcripts per Million mapped reads (RPKM) in the FLM (free living mycelium) and the ECM (Ectomycorrhizae).

Supplementary Table S4: Molecular analysis of *Laccaria bicolor MiSSP8*-RNAi lines. Molecular analysis of the four RNAi lines generated expressing RNAi hairpin targeting the MiSSP8 encoding transcript.

Supplementary File S1: Peptidase domain validation by PSI-Search. The protein sequence of the proteins from the white rot fungus *Schizophyllum commune* (JGIv3 H4-8 ID : #2745165, #112143, #2613917) were scanned using the PSI-Search server against the Uniprot-Database with default parameters (PSSM e-value cut-off: $1.0e^{-3}$).

(a)

(b)

(c)

(d)

(a)

(b)

(c)

Legend

Species / Protein ID — Size (amino acids)

- Signal Peptide
- DWRR motif
- Protein sequence

Species / Protein ID
Laccaria bicolor / 388224 / MiSSP8
Hebeloma cylindrosporum / 440029
Laccaria amethystina / 676588
Laccaria amethystina / 1718616
Hebeloma cylindrosporum / 448789
Laccaria bicolor / 334723
Hebeloma cylindrosporum / 443466
Paxillus ammoniavirescens / 1012017
Cortinarius glaucopus / 7098042

Ectomycorrhizal

Species / Protein ID
Gloeophyllum trabeum / 109288
Neolentinus lepideus / 1095641
Plicaturopsis crispa / 180022
Gloeophyllum trabeum / 141070

Brown rot

Species / Protein ID
Schizophyllum commune H4-8 / 2745165 (Peptidase A1 domain)
Schizophyllum commune Loenen D / 256147
Schizophyllum commune Tattone D / 324408
Gymnopus androsaceus / 1690366
Schizophyllum commune H4-8 / 2611276
Hypholoma sublateritium / 40934
Schizophyllum commune / 2613917 (Peptidase A1 domain)
Schizophyllum commune Tattone D / 112143 (Peptidase A1 domain)
Artolenzites elegans / 806214
Gymnopus androsaceus / 921359
Hypholoma sublateritium / 49943
Pycnoporus coccineus / 880174
Fistulina hepatica / 75093
Schizophyllum commune Loenen D / 248517
Schizophyllum commune Loenen D / 285556
Hypholoma sublateritium / 36958
Gymnopus androsaceus / 876936
Punctularia strigosozonata / 115989
Artolenzites elegans / 1302180
Pycnoporus coccineus / 1438311
Armillaria gallica / 1016168
Schizophyllum commune H4-8 / 2705922
Galerina marginata / 204523

White rot

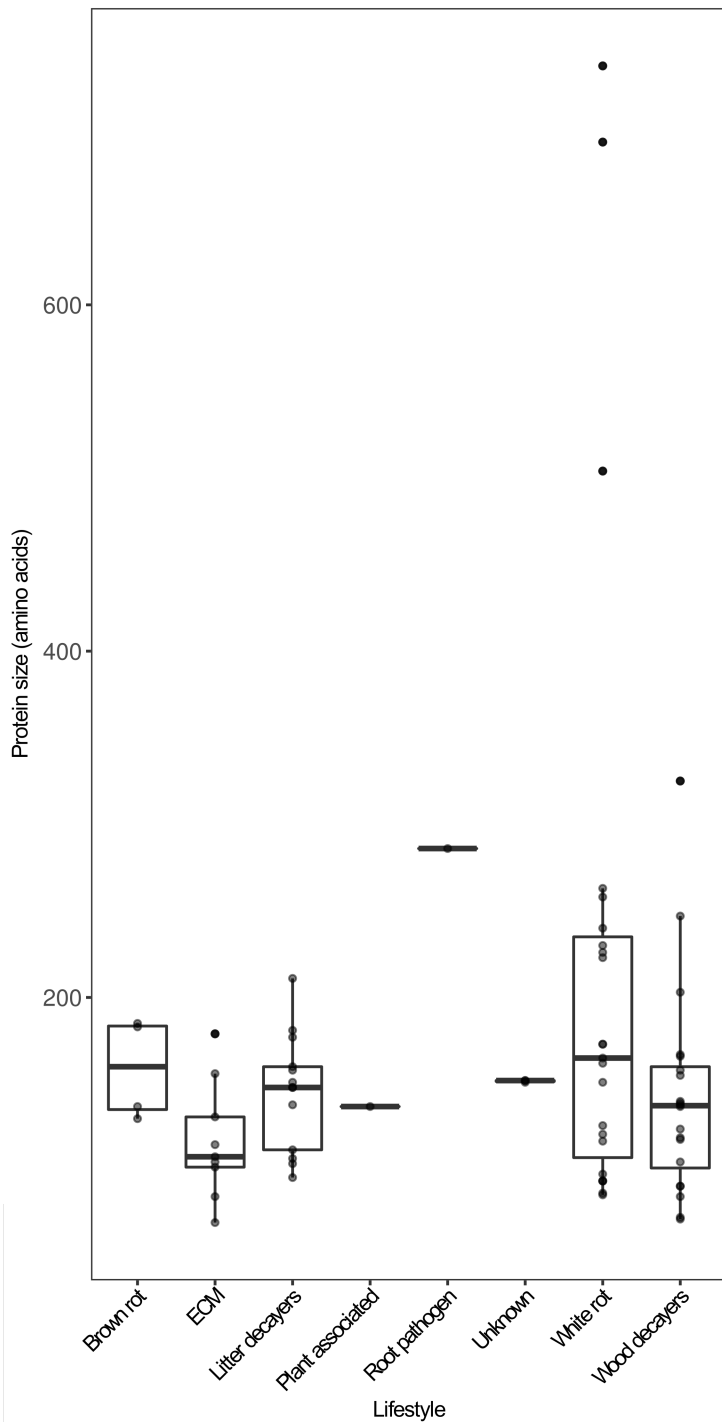| Species / Protein ID |
|---|
| *Amanita thiersii* / 5213 |
| *Gymnopus luxurians* / 239794 |
| *Macrolepiota fuliginosa* / 788375 |
| *Gymnopus luxurians* / 98464 |
| *Coprinopsis cinerea* / 9825 |
| *Amanita thiersii* / 46935 |
| *Agaricus bisporus* / 194352 |
| *Gymnopus luxurians* / 242026 |
| *Macrolepiota fuliginosa* / 735395 |
| *Pleurotus ostreatus* / 1091723 |
| *Coprinopsis cinerea* / 490115 |

Litter decayers

Species / Protein ID
Auriscalpium vulgare / 1681041
Botryobasidium botryosum / 36113
Bjerkandera adusta / 38578
Aporpium caryae / 771601
Sarcoscypha coccinea / 460438
Trematosphaeria pertusa / 507338
Ramaria rubella / 1624630
Auriscalpium vulgare / 1564130
Auriscalpium vulgare / 1678228
Rhizodiscina lignota / 58893
Macroventuria anomochaeta / 451518
Exidia glandulosa / 774536
Stereum hirsutum / 107311
Microstromatales sp / 278564
Bjerkandera adusta / 187723
Aporpium caryae / 735414
Schizopora paradoxa / 936356
Auriscalpium vulgare / 1681064
Aporpium caryae / 356713
Exidia glandulosa / 642657
Exidia glandulosa / 759788
Exidia glandulosa / 774536

Wood decayers

Species / Protein ID
Ceratobasidium sp / 609397

Plant associated

Species / Protein ID
Armillaria mellea / 13461

Root pathogen

Species / Protein ID
Dendrothela bispora / 800387
Dendrothela bispora / 807090
Dendrothela bispora / 836685

Unknown lifestyle

(a)

MiSSP8::eGFP   PDCB1::mCherry   Merged

(b)

ΔSP-MiSSP8::eGFP   ΔSP-MiSSP8::eGFP   PDCB1::mCherry   Merged

(c)

ΔSP-MiSSP8::eGFP   Aniline blue   Merged